Proceedings of the 2006 IEEE International Conference on Robotics and Automation
Orlando, Florida - May 2006

Graphical Singularity Analysis of Planar Parallel Manipulators

Amir Degani
[a]The Robotics Institute
Carnegie Mellon University
Pittsburgh PA 15213, USA
degani@cmu.edu

Alon Wolf[a]
Dept. of Mechanical Engineering
Technion Israel Institute of Technology
Technion City, Haifa 32000, Israel
alonw@tx.technion.ac.il

***Abstract* - This paper introduces a new approach to identify singularities of planar parallel manipulators (PPMs). This method is based on Maxwell's reciprocal figure theory which establishes a duality between self stressed frameworks and reciprocal figures, which are abstract dual representations of frameworks. We use line geometry tools to introduce a new graphical construction called the *Mechanism's Line of action Graph (MLG)*. The MLG is introduced in order to implement Maxwell's reciprocal figure theory to mechanisms. We show that the configurations where the MLG has a connected reciprocal figure imply a singularity in the mechanism. This singularity analysis tool is also used to trace the singularity loci of the PPM. Finally, we provide detailed examples of the singularity analysis of two common PPMs; one consists of three limbs with a passive revolute joint, actuated prismatic joint and another passive revolute joint (3-RPR), the other consists of three limbs with three revolute joints, where only the first is actuated (3-RRR).**

Index Terms - Graphical Analysis, Maxwell's Reciprocal Figure Theory, Parallel manipulators, Singularity.

I. INTRODUCTION

Parallel manipulators have various advantages over serial robots, such as high payload-to-weight ratio, high accuracy, and high rigidity. However, they also have a few drawbacks such as a relatively small workspace, relatively complex kinematics and most importantly, a failure while in, or close to singular configurations. In these configurations, the mechanism tends to lose its stiffness while gaining extra degrees of freedom (DOF) [1]. Physically, when the mechanism is in a singular configuration, the structure cannot resist or balance an external wrench applied to the end-effector (mobile platform), therefore may collapse.

This paper focuses on planar parallel manipulators (PPMs) and specifically on fully parallel planar manipulators which are planar 3-DOF parallel manipulators, consisting of three limbs, each consisting of one actuated joint and two unactuated (passive) joints. Different approaches have been applied to identify singular configurations of PPMs, using analytical, numerical and line geometry perspectives. These approaches address the singularity types that were introduced by Gosselin and Angeles [2]. These types are based on the singularity of the Jacobian matrix, which maps the Cartesian velocities of the end-effector onto the joint velocity vector. The instantaneous kinematics of a fully PPM is described by: $A\dot{x} = B\dot{q}$, where A and B are 3×3 Jacobian matrices. Type-I singularity (Inverse Kinematics singularity) occurs when $\det(B) = 0$. Type-II singularity (Direct Kinematics singularity) occurs when $\det(A) = 0$.

The method of investigating the Jacobian matrix analytically was extensively implemented on PPMs [3, 4]. Collins and McCarthy's investigation of the singularity of a PPM supported by three linear actuators resulted in an algebraic equation of a surface of points in projective plane for which the Jacobian is singular [3]. Further use of the analytic method was done to derive the singularity loci of planar parallel manipulators by using an algorithm that determines all of the configurations where the manipulator's Jacobian matrix is singular [5, 6]. Numerical procedures have been developed [7] in order to overcome the complexity involved in finding the singularity loci analytically, which even for the relatively simple PPMs may result in a high-order polynomial [6].

Line geometry tools were also used as a means to determine the singular configurations of parallel manipulators. It has been shown that the columns of the Jacobian matrix are zero-pitch or infinite-pitch wrenches (i.e. pure forces or pure torques) acting on the moving platform [8, 9]. Based on line variety and line dependency investigations [10] the singularity of parallel manipulators was interpreted as the configuration where the lines of actions are linearly dependent (e.g. [8, 9, 11]). Line geometry was also used to map singularity of different types of PPMs [12, 13].

We confront the problem of finding the singularities of PPMs somewhat differently. By building a graphical representation of the manipulator and locating special configurations which are the "graphical singularities", we are able to graphically locate singular configurations of the manipulator.

We first represent the manipulator graphically using a known line geometry tool, the *reciprocal screw*. This screw, which is reciprocal to all the unactuated joint twists of the limb, represents the *line of action* of a limb. This line of action represents the wrench that a limb applies to the end-effector. We represent the line of action of each limb of the manipulator as an edge in the *Mechanism's Line of action Graph (MLG)*. Then, in order to find the "graphical singularities" we use a theory that goes back to the mid 19th century, Maxwell's *reciprocal figure theory* [14], to construct

a dual graph (reciprocal figure) of the MLG. Maxwell's reciprocal figure theory was originally used to graphically analyze structures such as buildings and bridges, and to find the correct construction in which these structures are in self stress. Self stress is the state of a bar-joint framework for which the vector sum of the forces in the edges joining any joint is equal to zero. Note that the self stress state is usually desired for structures but not desired in mechanisms which also include actuators. We will show that this self stress state in a mechanism implies a dependency between the actuating wrenches of the mechanism which causes the mechanism to be in a singular configuration.

Our objective in this paper is to show the steps for graphically analyzing singular configurations of PPMs. We begin by constructing a graphical representation of the manipulator, and use Maxwell's reciprocal figure theory to construct the MLG's dual (reciprocal) graph. By checking, for a given configuration of the PPM, if the reciprocal figure is connected we locate the singular configurations of the PPM. A different starting point of the analysis is with a connected reciprocal figure upon which the MLG is built. In this type of analysis, when the configuration of the reciprocal figure is changed (while still being connected), the corresponding manipulator will change configuration but will continuously be in a singular configuration, resulting in the PPMs singularity loci.

II. Related Background and Tools

A. Reciprocal Screws and the Line of Action of a Limb

Finding the line of action for each limb of the manipulator is the first step in constructing the MLG. We use reciprocal screws to find these lines of action. The concept of reciprocal screws was first studied by Ball [15], followed by Hunt [16] and Roth [17]. Mohamed and Duffy [18] were the first to use reciprocal screws as an analysis tool for instantaneous kinematics. Later on, Tsai developed a specific procedure for the derivation of reciprocal screw and its application for the Jacobian analysis of parallel manipulators [19]. Bonev used derivations of reciprocal screws in the specific case of PPMs [12], which is relevant for the current analysis.

This paper focuses on 3-DOF fully parallel planar manipulators. A PPM is *fully parallel* if it is constructed of three limbs, each consisting of two unactuated joints and one active joint. The ith limb of the manipulator can be treated as a serial chain connecting the moving platform to the fixed base by three 1-DOF joints. The linear combination of the twists of these three joints for a limb results in the instantaneous twist of the moving platform, $\$_p$. Let $\hat{\$}_{j,i}$ be a unit screw associated with the jth joint of the ith limb and $\dot{\theta}_{j,i}$ denote the joint rates. The instantaneous twist of the moving platform $\$_p$ can be expressed as [18, 19]:

$$\$_p = \sum_{j=1}^{3} \dot{\theta}_{j,i} \hat{\$}_{j,i} \quad \text{, for any limb of the PPM } i = 1,2,3 \qquad (1)$$

In order to obtain the relationship between the instantaneous twist of the end-effector and the active joints of a limb we eliminate the unactuated joint twists by multiplying both sides of (1) (using the reciprocal product [16]) with a reciprocal screw $\$_r$ that is reciprocal to the two unactuated joints of the ith limb. This reciprocal screw, $\$_r$, is a wrench which if applied to the platform, can be resisted solely by the actuated joint of the limb. This reciprocal screw is the line of action of the ith limb, also known as the governing line of the limb [11, 12, 16, 19].

The lines of action of different limbs of a PPM depend on the combination of the unactuated joints of the limb. The two most common cases of unactuated joints in a PPM's limb are either two revolute joints or one revolute joint and one prismatic joint. A third, less common case, is a limb consisting of two passive prismatic joints. In the case of two revolute joints, the reciprocal screw is a pure force (zero pitch screw) passing through the two unactuated revolute joints (Fig. 1a,b,c). In the case of one revolute and one prismatic passive joints, the screw is a pure force passing through the unactuated revolute joint and perpendicular to the unactuated prismatic joint (Fig. 1d,e). Fig. 1a and Fig. 1b have a similar kinematic chain, however they differ in the location of the actuated joint (solid circle), which changes the line of action of the limb and therefore its corresponding reciprocal screw (marked as a dotted arrow). The limbs in Fig. 1c-f consist of prismatic joints. In Fig. 1c the prismatic joint is active and the other two are passive revolute joint and therefore the reciprocal screw is in the direction of the prismatic joint. In Fig. 1d,e on the other hand, the limbs consist of a passive prismatic joint and therefore the reciprocal screw is perpendicular to it. In the case of a limb consisting of two passive prismatic joints, the line of action is a pure torque in the direction perpendicular to the plane (Fig. 1f), and will only enable a pure torque and will not enable other movements of the PPM in the plane. For this reason, only one such limb can be included in the design of a PPM.

B. Maxwell's Reciprocal Figure Theory

In the mid 19th century James Clerk Maxwell described a 3-way connection between self stress in planar bar-joint frameworks (static rigidity), reciprocal figures, which are dual figures of the bar framework, and spatial polyhedra [14, 20]. This theory predicts configurations in which bar-joint frameworks are in self stress. Structural engineers, in fact, applied Maxwell's theory to the analysis of the Eiffel Tower built in 1889 [21]. For our purposes, we only focus on the first two components of the theory, i.e. the connection between a self stressed framework and the reciprocal figure.

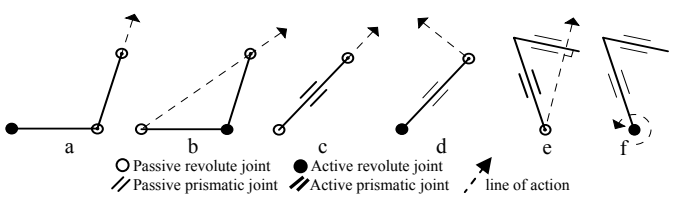

Fig. 1. Examples of typical limbs of PPMs and their reciprocal screws (dotted arrows) corresponding to the lines of action.

1) Bar-Joint Framework and Self Stress

A bar framework, $G(\mathbf{p})$, in the plane is a finite graph with vertices V, edges E, and a mapping $\mathbf{p}: V \to \mathbb{R}^2$. $\mathbf{p}(a)$ is the position of the vertex in the plane. The vertices of the graph correspond to the joints of the framework, i.e. $\mathbf{p}_i$ is the i^{th} joint. A bar connecting joints $\mathbf{p}_i$ and $\mathbf{p}_j$ is $\mathbf{p}_i - \mathbf{p}_j$. Let ω_{ij} be the magnitude of the force in the bar where $\omega_{ij} \geq 0$ represents tension and $\omega_{ij} \leq 0$ represents compression. The forces exerted by such a bar in tension (or compression) are forces along the line of the bar, equal in magnitude, but opposite in direction at the two ends, i.e.:

$$\omega_{ij}(\mathbf{p}_j - \mathbf{p}_i) \text{ at } \mathbf{p}_i \text{ and } \omega_{ij}(\mathbf{p}_i - \mathbf{p}_j) \text{ at } \mathbf{p}_j . \quad (2)$$

The forces reach equilibrium at the joint $\mathbf{p}_i$ if the sum of the forces in j bars connected to the joint $\mathbf{p}_i$ is equal to zero:

$$\sum_j \omega_{ij}(\mathbf{p}_j - \mathbf{p}_i) = 0 . \quad (3)$$

A self stress in a bar framework $G(\mathbf{p})$ is an assignment of scalars ω_{ij} to the edges such that, for each vertex $\mathbf{p}_i$, (3) is realized.
A framework is fully self stressed if for all ω_{ij}, $\omega_{ij} \neq 0$.

2) Maxwell's Reciprocal Figure Theory

The connection between self stress in frameworks and reciprocal figures was introduced by Maxwell [14]:

Theorem 2.1 Maxwell's Reciprocal figure theory:
A planar bar and joint framework, which is vertex 2-connected and edge 3-connected, supports a full self stress if and only if it has a reciprocal framework.

A graph is vertex 2-connected if removing any one vertex and its edges leaves the vertex set connected by the remaining edges and is edge 3-connected if removing any two edges leaves the vertex set connected by the remaining edges.

For each vertex in a full self stressed framework (3) can be geometrically represented as a closed polygon of forces. If we cycle around each vertex, placing the vectors $\omega_{ij}(\mathbf{p}_i - \mathbf{p}_j)$ end to end, a closed polygon is formed. Fitting these polygons together constructs a dual graph called the reciprocal figure (or the reciprocal graph).

Definition 2.1 Reciprocal Figure (graph) [14]:
Two graphs are reciprocal when they consist of an equal number of edges, so that corresponding edges in the two graphs are perpendicular, and corresponding lines which converge to a point in one graph form a closed polygon in the other.

This connection between reciprocal figure and self stress in a framework is the foundation to the connection we present between reciprocal figure and singularity type-II of a PPM. For more recent definitions, additional insights and a complete proof of Maxwell's reciprocal figure theory we refer the reader to [22].

III. Singularity Analysis Method and Examples

When using the graphical singularity analysis method presented in this paper one should apply the following three main steps on a given PPM:

STEP 1: Construct an MLG for the specific PPM.
STEP 2: Construct a reciprocal graph based on the MLG obtained in step 1.
STEP 3: Find the configurations of the manipulator in which the reciprocal graph is connected. In these configurations the manipulator is in type-II singularity.

As mentioned earlier, we conduct our investigation on fully parallel planar manipulators which consist of three limbs, each containing one actuated joint and two unactuated (passive) joints. Even though the examples provided in this paper are of identical limb manipulators, the method can be applied to different types of PPMs. We use the conventional notations of PPMs by using R to describe revolute joints and P to describe prismatic (linear) joints. Actuated joints are marked with an underline. When the three limbs of the PPM are identical the manipulator is marked by a preceding '3' (for example: 3-RRR).

A. Constructing the MLG of PPMs

Given a PPM we represent its kinematic structure in a graphical representation which mainly represents the line of action of each of the limbs of the PPM. This graphical representation is then used as a planar graph with Maxwell's reciprocal figure theory. In order to construct the Mechanism's Line of action Graph (MLG) we identify the reciprocal screw for each of the limbs of the PPM (as described in Section II.A).

The three limbs of a PPM can be connected to the end-effector either by revolute joints or by prismatic joints. This difference will affect the construction of the MLG. To begin an MLG construction of a PPM connected with revolute joints (Fig. 2a), the three vertices of the end-effector should be marked (Fig. 2b). From each of the end-effector's vertices an edge corresponding to the line of action of the limb is constructed. Fig. 2c illustrates the three reciprocal screws corresponding to the line of action of each limb (marked as dotted arrows). Even though the length of the edge corresponding to the line of action is not essential for this method, we draw the length of the edge equal to the length of the link closest to the end-effector (Fig. 2d). Finally, the three ground vertices of the line of actions' edges are to be connected (Fig. 2e). The ground vertices are located at the distal end of the line of action's edge with respect to the end-effector.

The MLG is changed depending on the configuration of the manipulator. In most PPMs, the ground vertices in the MLG are not static (as in the case of the 3-RRR in Fig. 2). This does not affect our results because we are only analyzing the instantaneous kinematics of the manipulator's end-effector. A similar step by step construction of an MLG of a 3-RPR is shown in Fig. 3.

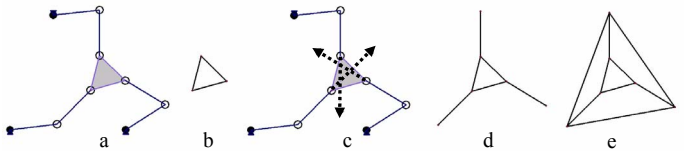

Fig. 2. Example of the construction of the MLG for a 3-RRR manipulator

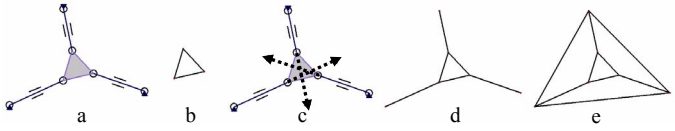

Fig. 3. Constructing the MLG for a 3-RPR manipulator

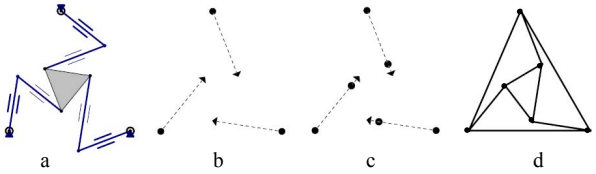

Fig. 4. Example of the construction of the MLG for a 3-RPP manipulator

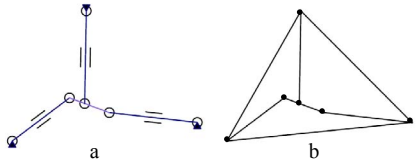

Fig. 5. Construction the MLG for a 3-RPR manipulator with degenerate end-effector

The main difference between the two MLGs in Fig. 2e and Fig. 3e is the line of action of each limb. In Fig. 3 the reciprocal screws that correspond to the lines of action of the limbs pass through the center of the passive revolute joints of the limb (first and third joints). In Fig. 2 the lines of action pass through the second and third joints which are the passive ones.

In the case of a limb connected to the end-effector by prismatic joints (Fig. 4a), the construction of the MLG should begin from the ground vertices. First the three ground vertices are constructed. From each of the ground vertices an edge corresponding to the line of action of the limb is constructed (Fig. 4b). Three vertices are constructed on each of the edges corresponding to the line of action at a constant, arbitrary unit distance from the ground vertex (Fig. 4c). Connecting these three vertices and the three ground vertices finalizes the construction of the MLG (Fig. 4d).

An example of a degenerate case of a PPM's end-effector, in which the three distal joints create a line, is shown in Fig. 5a. To construct an MLG for this special case the end-effector should still be thought of as a triangle in a degenerate configuration (Fig. 5b). It is important to note that currently it is not feasible when using this method to represent the line of action of a limb consisting of two passive prismatic joint in an MLG (i.e. a pure torque out of the plane) as in Fig. 1f.

B. Constructing a reciprocal graph of the PPM's MLG

As mentioned earlier, the MLG is constructed based on the momentary PPM configuration. This graphical representation enables us to construct Maxwell's reciprocal figure. Following Definition 2.1, one can build the reciprocal figure for any configuration of the MLG. We use a dynamic geometry program that enables us to construct the reciprocal figure for a given configuration so that when the mechanism is moved, the reciprocal figure will respectively change. We note that these constructions can be drawn using a simple ruler and a compass (most likely the tools that the late Maxwell originally used), but for every different configuration, a new reciprocal graph should be drawn. Fig. 6 presents a step by step construction of the reciprocal figure of the 3-RPR's MLG. The MLG that was constructed for the 3-RPR PPM in Fig. 3, is given in Fig. 6a. To start the construction of the reciprocal figure an arbitrary inner polygon in the MLG is picked (polygon (1,2,3,4)). An initial vertex is drawn and the four perpendicular lines corresponding to the polygon's edges are constructed (Fig. 6b). Then another vertex is drawn on line (4) since its corresponding edge is shared by the top two inner polygons in the MLG. Next, the three perpendicular lines corresponding to the remaining edges of the top right polygon in the MLG (edges 5, 6, and 7) are constructed (Fig. 6c). The reciprocal graph should eventually consist of edges and not infinite lines. In order to correctly trim the lines we have constructed we need to determine the intersections that are actually vertices that correspond to closed polygons in the MLG. The intersections that join lines correspond to edges of the closed polygons that have not yet been addressed need to be marked, i.e. the bottom polygon, the center triangle and the outer triangle. In Fig. 6d the three vertices are marked (3/7, 1/5, 6/2). For example the 1/5 vertex corresponds to the 1,4,3,2 polygon, and so forth. After marking these vertices the reciprocal figure can be "cleaned" and infinite lines can be trimmed (Fig. 6e). To finalize the construction of the reciprocal figure, edges 8 and 9 (from the bottom polygon) should be added to the bottom vertex of the reciprocal figure, perpendicular to their corresponding edges (Fig. 6f). Note that

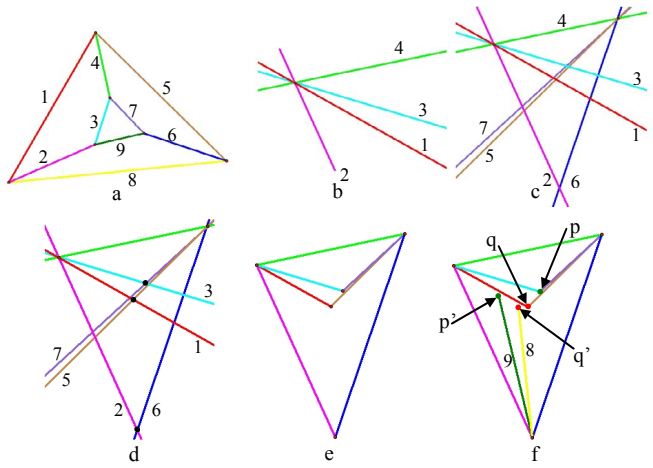

Fig. 6. Construction of the reciprocal figure for a 3-RPR PPM

these two edges (8, 9) are not connected to their correct vertices (vertices p and q). This means that for this particular configuration, a connected reciprocal figure does not exist. Therefore, the specific configuration of the PPM (Fig. 3a) for which this MLG was constructed (Fig. 3e), is not a type-II singularity. We note that the order in which we construct the reciprocal figure may change the resulting edges that are not connected; however, this does not change the overall connectivity status of the reciprocal figure. The construction of the reciprocal figure for the 3-RRR manipulator is done in a similar way.

The construction of the degenerate end-effector (Fig. 5) can also be constructed in a similar way, while keeping in mind that the three joints (in this case on a line) are in fact a degenerate triangle. In this case three of the edges of the reciprocal figure will always be parallel to each other and will always coincide at infinity. The remaining edges will therefore determine the connectivity status of the reciprocal figure.

C. Duality between type-II singularity in PPMs and self stressed frameworks

Once the MLG of a PPM and a reciprocal figure are constructed, one can use them for the singularity analysis of PPMs. Maxwell's theory (Theorem 2.1) presents a connection between the existence of a connected reciprocal figure and self stress in a framework. We will now analyze a self stressed MLG (Fig. 7) in order to demonstrate the connection between self stress and singularity. Based on the definition of self stressed framework, when a bar-joint framework is in self stress, the sum of the forces of the bars connected to a joint is equal to zero. Three equations corresponding to the sum of forces in the three vertices 1,2,3 can be written as:
The sum of forces in vertex 1:

$$\mathbf{a} + \mathbf{d} + \mathbf{f} = \mathbf{0}, \quad (4)$$

the sum of forces in vertex 2:

$$\mathbf{b} - \mathbf{d} + \mathbf{e} = \mathbf{0}, \quad (5)$$

and the sum of forces in vertex 3:

$$\mathbf{c} - \mathbf{e} - \mathbf{f} = \mathbf{0}. \quad (6)$$

These three equations are vector summations. We arbitrarily assign the direction of the forces and consistently add the forces. Therefore, some of the forces in (4)-(6) are negated.
Summing (4), (5), and (6):

$$\mathbf{a} + \mathbf{b} + \mathbf{c} = \mathbf{0}. \quad (7)$$

Equation (7) is a linear dependency of the three forces $\mathbf{a}$, $\mathbf{b}$, and $\mathbf{c}$. These three forces are the forces corresponding to the lines of actions of the three limbs. The meaning of this dependency is that these three limbs cannot generate instantaneous work (virtual work [16]) on the end-effector while it is moving in an instantaneous twist deformation resulting from an external wrench applied on it. Therefore, self stress in a framework is equivalent to a type-II singularity of a PPM. It is now evident that the existence of a connected reciprocal figure indicates a self stressed framework, and in a similar way indicates a singular configuration in a mechanism.

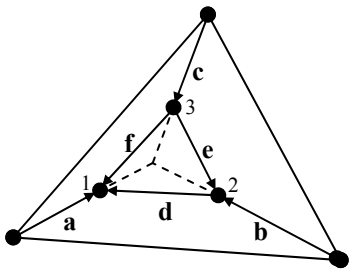

Fig. 7. "Singular" (self stress) configuration of MLG

D. Locating the singular configurations

To find the configurations where there exists a connected reciprocal figure to a particular PPM, and therefore it is in a singular configuration, one should move the manipulator by changing its joint parameters while tracking for configurations in which the reciprocal figure is visually connected. Fig. 8 and Fig. 9 show examples of PPM configurations in which the reciprocal figures are connected and the manipulators are in fact in type-II singular configurations.

So far the search for a singular configuration was carried out by changing the joint parameters of the manipulator and checking for the existence of a connected reciprocal figure. If the analysis is constructed the other way around, so that a connected reciprocal figure is first constructed and only then an MLG is constructed to be reciprocal to it, we can trace the loci of the singular configurations of the manipulator by changing the reciprocal figure while keeping it connected (Fig. 10). Note that the construction of the reciprocal figure in this case is based on mechanical constraints of the PPM, e.g. the fixed shape of the end-effector. Moreover, the singular configuration's loci are traced relative to a constant orientation of the PPM in order to enable us to plot the loci as a 2-D graph. Fig. 11 shows the singularity loci of a 3-RPR PPM in six different constant orientations of the end-effector. We refer the readers to [5] to examine the resemblance of the results. More examples, including JAVA applets of this method, can be found at: www.cs.cmu.edu/~adegani/graphical

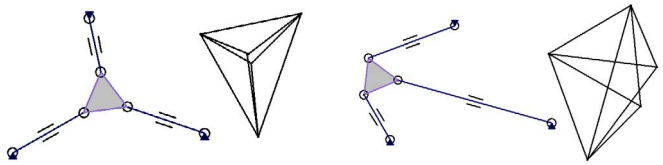
Fig. 8. Two examples of singular configurations of the 3-RPR Manipulator and the connected reciprocal figures

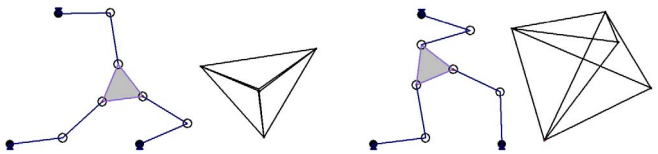
Fig. 9. Two examples of singular configurations of the 3-RRR Manipulator and the connected reciprocal figures

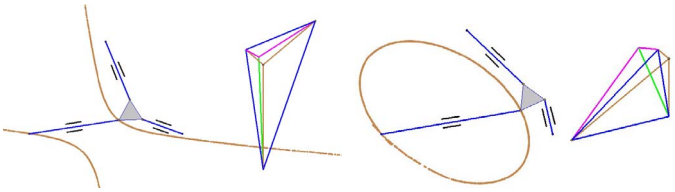

Fig. 10. Singularity Loci of 3-RPR manipulator in two different constant orientations of the end-effector

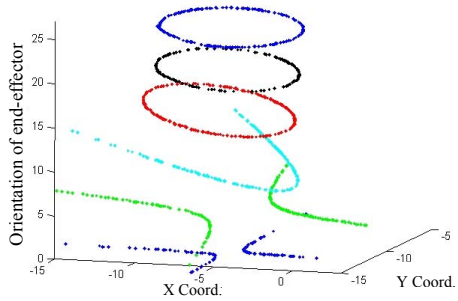

Fig. 11. Singularity loci of 3-RPR in different constant orientations of the end-effector (0,5, 10, 15, 20, and 25 degrees)

V. Future Work

As we have shown, our method enables graphical analysis of the singular configurations of fully PPMs. It also enables to trace the singularity loci of the PPM by systematically searching the configuration space of the reciprocal figure. A possible future direction would be to apply this method to other mechanisms such as redundant PPMs. We are currently facing the challenge of expanding this graphical method to the analysis of 3-dimensional manipulators. We hope to be able to use our relatively simple method to find the singular configurations of complex 3-dimensional manipulators, such as a 6-DOF Gough–Stewart platform. One possible way to achieve this goal is to project the 3-dimensional lines of action of the limbs on one or more planes [23]. We believe a self stress analysis of these projected graphs, similar to the one done on PPM, will offer insight into the singular configurations of these non-planar manipulators.

VI. Conclusions

The graphical method that is presented and implemented in this paper results in comparable outcomes to those obtained by other approaches (e.g. [5] and [6]), yet avoids some of the complexities involved in analytic derivations. It is worth mentioning that the method we present can potentially be applied to non-identical limb manipulators and to other types of mechanisms as well. The method makes use of reciprocal screws to represent the lines of actions of PPMs' limbs in a Mechanism's Line of action Graph (MLG), an insightful graphical representation of the mechanism. Maxwell's theory of reciprocal figure and self stress is then applied to create a dual figure of the MLG. Analyzing this dual (reciprocal) figure provides us with the singular configurations of the PPM and with the loci of singular configurations of the manipulator.

References

[1] K. H. Hunt, "Structural kinematics of in-parallel actuated robot arms," *J. Mech. Transm.-T. ASME*, vol. 105, no. 4, pp. 705-712, 1983.

[2] C. Gosselin and J. Angeles, "Singularity analysis of closed-loop kinematic chains," *IEEE T. Robotic. Autom.*, vol. 6, no. 3, pp. 281-290, 1990.

[3] C. L. Collins and J. M. McCarthy, "Quartic singularity surfaces of planar platforms in the Clifford algebra of the projective plane," *Mech. Mach. Theory*, vol. 33, no. 7, pp. 931-944, 1998.

[4] G. Yang, I. M. Chen, W. Lin, and J. Angeles, "Singularity analysis of three-legged parallel robots based on passive-joint velocities," *IEEE T. Robotic. Autom.*, vol. 17, no. 4, pp. 413-422, 2001.

[5] J. Sefrioui and C. M. Gosselin, "On the quadratic nature of the singularity curves of planar three-degree-of-freedom parallel manipulators," *Mech. Mach. Theory*, vol. 30, no. 4, pp. 533-551, 1995.

[6] I. A. Bonev, D. Zlatanov, and C. M. Gosselin, "Singularity loci of planar parallel manipulators with revolute joints," in 2nd Workshop on Computational Kinematics (CK2001), 2001, pp. 291–299.

[7] F.-C. Yang and E. J. Haug, "Numerical analysis of the kinematic working capability of mechanisms," *J. Mech. Design.*, vol. 116, pp. 111-118, March 1994.

[8] J.-P. Merlet, "Parallel manipulators. Part 2: Theory. Singular configurations and Grassmann geometry," INRIA, Le Chesnay Cedex, Technical Report 791, 1988.

[9] C. L. Collins and G. L. Long, "Singularity analysis of an in-parallel hand controller for force-reflected teleoperation," *IEEE T. Robotic. Autom.*, vol. 11, no. 5, pp. 661-669, Oct. 1995.

[10] A. Dandurand, "The rigidity of compound spatial grids," *Structural Topology*, vol. 10, pp. 41–56, 1984.

[11] N. Simaan and M. Shoham, "Singularity analysis of a class of composite serial in-parallel robots," *IEEE T. Robotic. Autom.*, vol. 17, no. 3, pp. 301-311, June 2001.

[12] I. A. Bonev, *Geometric analysis of parallel mechanisms*,Ph.DThesis, Laval University Quebec, QC, Canada, 2002.

[13] I. A. Bonev, D. Zlatanov, and C. M. Gosselin, "Singularity analysis of 3-DOF planar parallel mechanisms via screw theory," *J. Mech. Design.*, vol. 125, no. 3, pp. 573-581, 2003.

[14] J. C. Maxwell, "On reciprocal figures and diagrams of forces," *Phil. Mag*, vol. 4, no. 27, pp. 250-261, 1864.

[15] R. S. Ball, *A treatise on the theory of screws*, Cambridge: Cambridge University Press, 1900.

[16] K. H. Hunt, *Kinematic Geometry of Mechanisms*, Oxford: Clarendon Press, 1978.

[17] B. Roth, "Screws, motors, and wrenches that cannot be bought in a hardware store," in Robotics Research: The First International Symposium, 1984, pp. 679-693.

[18] M. G. Mohamed and J. Duffy, "Direct determination of the instantaneous kinematics of fully parallel robot manipulators," *J. Mech. Transm.-T. ASME*, vol. 107, no. 2, pp. 226-119, 1985.

[19] L. W. Tsai, "The Jacobian analysis of a parallel manipulator using reciprocal screws," in Proceedings of the 6th International Symposium on Recent Advances in Robot Kinematics, 1998, pp. 327-336.

[20] J. C. Maxwell, "On reciprocal figures, frames and diagrams of forces," *Trans. Royal Soc.*, vol. 26, pp. 1-40, 1870.

[21] T. M. Charlton, *A history of the theory of structures in the nineteenth century*, Cambridge: Cambridge University Press, 2002.

[22] H. Crapo and W. Whiteley, "Plane self stresses and projected polyhedra I: The basic pattern," *Structural Topology*, vol. 20, no. 1, pp. 55-78, 1993.

[23] A. Karger, "Projective properties of parallel manipulators," in *Advances in Robot Kinematics*, J. Lenarcic and C. Galletti, Eds. Sestri Levante, Italy, 2004, pp. 89-96.